



Published in final edited form as:

Radiat Environ Biophys. 2020 March ; 59(1): 89–98. doi:10.1007/s00411-019-00825-x.

DNA damage response in peripheral mouse blood leukocytes *in vivo* after variable, low-dose rate exposure

Qi Wang^{*}, Monica Pujol Canadell, Maria Taveras, Guy Garty, Jay Perrier, Carlos Bueno-Beti, Igor Shuryak, David J. Brenner, Helen C. Turner

Center for Radiological Research, Columbia University Irving Medical Center, New York, NY 10032, USA

Abstract

Environmental contamination and ingestion of the radionuclide Cesium-137 (¹³⁷Cs) is a large concern in fallout from a nuclear reactor accident or improvised nuclear device, and highlights the need to develop biological assays for low-dose rate, internal emitter radiation. To mimic low-dose rates attributable to fallout, we have developed a VArable Dose-rate External ¹³⁷Cs irradiator (VADER), which can provide arbitrarily varying and progressive low dose rate irradiations in the range of 0.1 to 1.2 Gy/day, while circumventing the complexities of dealing with radioactively-contaminated biomaterials. We investigated the kinetics of mouse peripheral leukocytes DNA damage response *in vivo* after variable, low-dose rate ¹³⁷Cs exposure. C57BL/6 mice were placed in the VADER over 7 days with total accumulated dose up to 2.7 Gy. Peripheral blood response including the leukocytes depletion, apoptosis as well as its signal protein p53 and DNA repair biomarker γ -H2AX were measured. The results illustrated that blood leukocyte numbers had significantly dropped by day 7. P53 levels peaked at day 2 (total dose= 0.91 Gy) and then declined, whereas γ -H2AX fluorescence intensity (MFI) and foci number generally increased with accumulated dose and peaked at day 5 (total dose= 2.08 Gy). ROC curve analysis for γ -H2AX provided a good discrimination of accumulated dose < 2 Gy and \geq 2 Gy, highlighting the potential of γ -H2AX MFI as a biomarker dosimetry in a protracted, environmental exposure scenario.

Terms of use and reuse: academic research for non-commercial purposes, see here for full terms. <https://www.springer.com/aam-terms-v1>

*Corresponding author: Qi Wang, qw2232@cumc.columbia.edu, Telephone: 212-305-7387.

Publisher's Disclaimer: This Author Accepted Manuscript is a PDF file of an unedited peer-reviewed manuscript that has been accepted for publication but has not been copyedited or corrected. The official version of record that is published in the journal is kept up to date and so may therefore differ from this version.

Ethics approval

All applicable international, national, and/or institutional guidelines for the care and use of animals were followed. All procedures performed in studies involving animals were in accordance with the ethical standards Columbia University Institutional Animal Care and Use Committee (IACUC, #AC-AAAQ2410).

Consent for publication

Not applicable

Availability of data and material

The data that support the findings of this study are available from the corresponding author upon reasonable request.

Competing interests

The authors declare that they have no competing interests.

Keywords

Biodosimetry; Cesium-137; Variable low-dose rate; protein p53; γ -H2AX

Introduction

The effect of internal emitters and associated varying dose rate effects on biodosimetry are not well studied. Cesium-137 (^{137}Cs), a fission product of uranium and plutonium, is a radionuclide of concern and major environmental contaminant following the detonation of an improvised nuclear device (IND) or a nuclear reactor accident (Garty et al. 2017; Simon et al. 2004; Yasunari et al. 2011). Researchers at the Lawrence Livermore laboratory have performed computer simulations to show prompt effects and fallout patterns from hypothetical INDs for a number of U.S. cities (Buddemeier and Dillon 2009; Heller 2015). The simulations showed that fallout decays rapidly over the first 7 hours (dose rate is ~ 1 Gy/h) followed by a slower decay and dangerous fallout zone up to 48 hours (radiation levels greater than 0.1 Gy/h). The primary hazard from fallout is not from breathing in radioactive particles but from exposure to particles that have settled on the ground and roofs (Buddemeier and Dillon 2009; Heller 2015). The Chernobyl and Fukushima Daiichi accidents illustrate the large-scale detrimental effects of the environmental radioactive contamination (López-Vicente et al. 2018; Moysich et al. 2002; Nakamura et al. 2017; Steinhausler 2005) whereby a significant amount of soluble radionuclides may be dispersed into the atmosphere as a component of fallout, and ingested or inhaled by vast numbers of people located at substantial distances from the radiological event site. Measurements of the DNA damage response observed at variable/decaying dose rate of ionizing radiation are important to the study of cell and tissue biological response after radiation exposure as well as the development biodosimetry system.

Compared with external exposure, the dose rates of internal exposures are typically much lower (below 1 Gy/day). At the Columbia University Center for High Throughput Minimally Invasive Radiation Biodosimetry in Center Medical Countermeasures against Radiation (CMCR), we have used a $^{137}\text{CsCl}$ internal emitter mouse model to examine the long-term effects of $^{137}\text{CsCl}$ activity for cytogenetic (Turner et al. 2015b), transcriptomic (Paul et al. 2014) and metabolomic (Goudarzi et al. 2013) endpoints. The challenge with using the ^{137}Cs injection mouse studies is that all the biomaterials are radioactively contaminated, and as such, requires dedicated equipment, costly clean-up and decontamination procedures. To overcome this drawback, we have developed a VARIable Dose rate External ^{137}Cs irradiator (VADER) to facilitate modeling of low dose rate ^{137}Cs exposure in mice using external irradiations. Based on the repurposing of using retired ^{137}Cs brachytherapy seeds, the VADER irradiator is designed to provide arbitrarily varying and constant low dose rate irradiations in the range 0.1-1.2 Gy/day, resulting in chronic exposures of Gy-level doses over days to weeks of exposure (Garty et al. 2019a; Garty et al. 2017). The advantages of such a system are that it allows for experiments in a controlled, non-radioactive setting which can be programmed to mimic internal ^{137}Cs biokinetics.

In our earlier work, we showed the persistence of radiation-induced DNA γ -H2AX double strand breaks (DSBs) *in vivo*, several weeks after the administration of ^{137}Cs internal emitter gamma radiation which is in clear contrast to acute dose exposures where the γ -H2AX is typically decayed after 24-48 h due to DSB repair (Redon et al. 2010; Rothkamm and Horn 2009; Turner et al. 2019; Turner et al. 2014). We injected C57BL/6 mice with a range of $^{137}\text{CsCl}$ activities to achieve total-body committed doses of ~ 4 Gy at specific time points up to 14 days of ^{137}Cs exposure. Despite the complicated nature of the studied biological system and the time-dependent changes in radiation dose and dose rate due to radionuclide excretion, we were able to profile γ -H2AX repair kinetics and develop a semi-empirical model for predicting initial ^{137}Cs incorporation activity, based on measurements 2-5 days after initial incorporation (Turner et al. 2019).

The objective of the present work was to extend the previous ^{137}Cs -injected mouse studies using our novel VADER irradiation system and measure the DNA damage response by imaging flow cytometry (Lee et al. 2019) in peripheral blood leukocytes upon progressively decreasing low-dose rate external exposures. The study was designed to expose C57BL/6 mice in VADER irradiation over 7 days (dose rate <0.5 Gy/day) with accumulated doses ranging from 0.49 Gy (day 1) to 2.68 Gy (day 7) and measure the following endpoints: 1) mouse leukocytes depletion, 2) apoptosis levels, 3) p53 expression and 4) γ -H2AX kinetics.

Materials and Methods

Experimental animals

The animal studies were approved by the Columbia University Institutional Animal Care and Use Committee (IACUC, #AC-AAAQ2410). All procedures performed in studies involving animals were in accordance with the ethical standards of IACUC. Male C57BL/6 mice (approximately 7 weeks old, 20-30 g) were purchased from Charles River Laboratories (Frederick, MD) and quarantined for a minimum of 14 days prior to group assignment by body weight stratification for randomization onto the study.

Irradiations and dosimetry

- i) The variable dose rate external ^{137}Cs irradiator (VADER)**—The VADER is a custom built irradiation system, built to deliver controlled dose rates in the range 0.1-1 Gy/day to a cohort of up to 15 mice. The VADER uses ~ 0.5 Ci of retired ^{137}Cs brachytherapy seeds, arranged in two platters, and placed above and below a “mouse hotel”. The sources can be moved under computer control to provide the required dose rate as a function of time. The VADER is shielded such that the dose rate in the room is <0.1 mGy/wk.
- ii) VADER mouse hotel setup**—The hotel consists of a 35 cm \times 35 cm \times 12 cm acrylic box with sufficient bedding material, which can house up to a total of 15 mice. Within the hotel, mice are free to move around, interact with each other, eat and drink *ad libitum*. Temperature, humidity, air flow and lighting are fully controlled to the required animal care standards. All these environmental controls and monitoring are integrated into a removable mouse hotel so that they can be easily replaced in case of radiation damage. To monitor the

environment in the mouse hotel, a temperature/humidity sensor (HWg HTemp, TruePath Technologies Victor, NY) is integrated into one of the hotel walls. Real time monitoring of the mice is performed using a 180° fisheye USB camera (ELP, Amazon) embedded into one of the hotel walls.

iii) Mouse TLD dosimetry—To identify the absorbed dose that each mouse received, *in vivo* dosimetry was performed on a mouse-by-mouse basis by injecting a glass encapsulated TLD chip into each mouse (Garty et al. 2019a). Anesthesia was induced with 2% isoflurane delivered in 100% oxygen for <3 min before the implantation procedure. The encapsulated TLD rods (one per mouse) were placed in a 12-gauge needle coupled with a needle injector (Allflex, Irving, TX) and administered by subcutaneous injection in the dorsal neck. Following implantation, mice were monitored up to 48 hours for complications. TLD rods were later read using a Harshaw 2500 TLD reader (Thermo Fisher Scientific™, Waltham, MA), most experiments used a heating profile consisting of a 5 °C/sec ramp up to 300 °C followed by a short hold at 300 °C and cool down to 50 °C. Dose was reconstructed based on the integrated light yield at a temperature higher than 180 °C to eliminate the low temperature, time dependent, glow peak (Garty et al. 2019b).

iv) VADER irradiation and dosimetry—The VADER was programmed to provide the dose rate profile for 2 batches of experiments shown in Fig. 1 with the source position updated hourly. This profile corresponds to the double exponential decay measured by Paul et al (Paul et al. 2014)

$$\text{dose rate} = \text{initial dose rate} \times (0.21e^{-1.0t} + 0.79e^{-0.096t})$$

The dose rate was converted to source retraction using the VADER calibration curve:

$$\text{dose rate}[\text{Gy/day}] = 0.102 + 1.55 \cdot 10^{-5} R + 1.26 \cdot 10^{-9} R^2 + 4.61 \cdot 10^{-14} R^3$$

Where R is the source position, with $R=0$ corresponding to the lowest dose rate of 0.1 Gy/day and $R=34,200 \text{ steps}$ corresponds to 1 Gy/day.

v) Mouse Irradiation—Two randomized batches of 15 mice were loaded in the VADER hotel for irradiation respectively as the maximum number of mice that VADER can house is 15 mice. The first batch of mice was irradiated for 3 days, 4 days and 7 days. The second batch of mice was irradiated for 1 day, 2 days and 5 days. Randomized control mice were housed in an identical hotel with monitor system. For each time/dose point, 5 irradiated mice and control mice were assigned. The temperature in the VADER and control cage was 20°C to 25°C. Humidity in both ranged from 40% to 60%.

Blood sample collection and cell counts

VADER-irradiated mice were sacrificed with paired non-irradiated sham-control mice on the same day after irradiation. All mice were euthanized by CO₂ asphyxiation prior to blood collection. Peripheral whole blood samples were collected from each mouse by cardiac puncture using a heparin-coated syringe. Leukocyte, T and B cell counts were determined by

flow cytometry using 20 μ L of heparinized blood following the standard flow cytometry surface staining protocol. Peripheral blood was surface stained with APC/Cy7 conjugated anti-mouse CD45 antibody (clone 30-F11, Biolegend, San Diego, CA), APC conjugated anti-mouse CD3 antibody (clone 145-201, Biolegend) and PE conjugated anti-mouse CD19 antibody (clone 6D5, Biolegend), lysed with FACS lysing solution (BD Biosciences, Franklin Lakes, NJ), washed in phosphate-buffered saline (PBS, Gibco, Waltham, MA) with 5% fetal bovine serum (FBS) and measured on flow cytometry with well-established compensated matrix (CytoFLEX, Beckman Coulter, Pasadena, CA). Analyses were performed using CytExpert Software (Beckman Coulter).

Imaging flow cytometry p53 and γ -H2AX analysis

Peripheral blood samples were lysed with RBC lysis buffer (Invitrogen™ Waltham, MA), fixed using the FIX & PERM™ Cell Permeabilization Kit (Thermo Fisher Scientific™, Waltham, MA), washed with perm/wash buffer from the kit, and stained intracellularly by a rabbit polyclonal γ -H2AX (Abeam, Cambridge, MA) or a rabbit polyclonal p53 (Phospho-Ser37, Aviva systems biology, San Diego, CA). Proper isotype controls were included for intracellular staining as negative controls (Abeam, Rabbit polyclonal IgG). Following washing, cells were stained with a goat anti-rabbit Alexa Fluor 488 secondary antibody (Life technology, Carlsbad, CA). Samples were then washed with PBS, stained with the nuclear dye DRAQ5 (Thermo Fisher Scientific™) and measured using the ImageStream®x MkII Imaging Flow Cytometer (LUMINEX Corporation, Austin, Texas). Images of more than 5000 cells per sample were acquired at 40 \times magnification using the 488 nm excitation laser. For the compensation, cells stained with γ -H2AX antibody, p53 antibody or DRAQ5 only were captured using the 488 nm laser with inactivated bright field illumination. The compensation coefficients were acquired automatically by the IDEAS 6.2 compensation wizard. Captured images were analyzed using IDEAS® (LUMINEX Corporation, Austin, Texas) software for measuring proportions of apoptotic cell; γ -H2AX and p53 mean fluorescence intensity (MFI) and γ -H2AX foci number.

Fig. 2 images a-d show the representative gating strategy to identify focused non-apoptotic cell population for measurement of fluorescence intensity of γ -H2AX and p53; images e-f show quantification of the γ -H2AX foci. The focused cells were gated according to the gradient similarity feature by visual inspection of cell images in the bright field channel (Fig. 2a). Single cells were then selected from images according to their area and aspect ratio in the bright field channel (Fig. 2b) and nucleated cells are selected based on DRAQ5 positivity to exclude the dead cells (Fig. 2c). As apoptotic cells showed a different pattern of γ -H2AX staining (Sober and Pommier 2014), they were then excluded according to the complexity of the nucleus and contrast of brightfield morphology (Fig. 2d). The MFI of γ -H2AX and p53 within the gated cells population was then analyzed and exported from the IDEAS® software. The γ -H2AX foci number was identified using the spot counting wizard (Fig. 2e). This wizard automatically creates masks based on peak mask identified intensity areas from an image with local maxima (bright) or minima (dark), followed by enumerate foci identified by the mask. Accuracy of foci identification by wizard was confirmed by visual inspections. Fig. 2f is a representative histogram for quantify foci number of each cell

in one sample. A template file was then generated and applied to all data files and automatically batch processed on IDEAS®.

Statistical analysis

Analyses were performed by GraphPad Prism version 6.00 for Windows (GraphPad Software Inc., La Jolla, CA). The Kruskal-Wallis test was used to compare data among all study groups and the Mann-Whitney U test was then used to compare between irradiated and control groups. The Spearman's rank correlation coefficient was used to assess accumulated dose dependence of the γ -H2AX levels (MFI and foci number). γ -H2AX performance was determined based on Receiver Operating Characteristic (ROC) curves, which allow the characterization of the discrimination between two well-defined populations. The sensitivity, specificity, positive and negative predictive values were evaluated using the optimal threshold value calculated to maximize the Youden's index. This index is defined as the sum of the sensitivity and specificity (both expressed by a number comprised between 0 and 1) minus 1 to set up the criterion for selecting the optimum cut-off point. All differences were considered statistically significant when $p < 0.05$.

Results

Mouse Dosimetry and Nominal dose

Fig. 3 shows the calculated dose rate, based on the measured source positions, as well as the cumulative dose for each of the two runs. The vertical dips correspond to VADER openings to extract mice.

Peripheral blood cell counts kinetics

The total number of peripheral blood leukocyte (CD45+), T cells (CD3+) and B cells (CD19+) were quantified by flow cytometry (Fig. 4). The total blood leukocyte count was not significantly different from non-irradiated controls until day 7 in the VADER irradiated group ($p < 0.01$) (Fig. 4a), as were the T cell counts ($p < 0.05$) (Fig. 4b). B cells responded with increased sensitivity to radiation whereby the number of cells had significantly decreased by day 4 and remained low up to 7 days (Fig. 4c).

P53 and γ -H2AX response

The overall rate of apoptotic cells identified by IDEAS® software based on their morphology and nuclear complexity was relatively low ($< 3\%$), with no significant difference observed between the VADER irradiation group and the non-irradiated control (data not shown). Activation of p53 protein in the cell nuclei of the non-apoptotic leukocyte population was also quantified. To compensate for the random measurement error, the non-irradiated mice p53 MFI were normalized to 1000 MFI units, and the VADER irradiated mice p53 MFI level were calculated based on the same-day non-irradiated control. The results show that p53 MFI peaked on day 2 and then declined, but remained significantly above non-irradiated baseline levels up to day 4 ($p < 0.05$, Fig. 5a).

Measurements of γ -H2AX MFI and foci number displayed a similar trend with increasing accumulated dose during the 7-day study period. For each time point, γ -H2AX MFI of non-

irradiated control mice was normalized to the average of 1000 unit of MFI. Foci number was normalized to the average of 5 per cell. The data are presented as the relative MFI (Fig. 5b) and foci number (Fig. 5c) compare with the same day non-irradiated control mice sample. For each time point, γ -H2AX MFI of non-irradiated control mice was normalized to the average of 1000 unit of MFI and foci number was normalized to the average of 5 per cell. The results show that that the γ -H2AX MFI and foci numbers are significantly increased by day 3 and peaked at day 5, after which time the γ -H2AX levels significantly decreased.

γ -H2AX MFI as a biodosimetry marker for the accumulated dose

Since γ -H2AX MFI and foci number showed a similar trend with accumulated dose, we performed the correlation of accumulated dose with γ -H2AX MFI and γ -H2AX foci number (Fig. 6). The data show that γ -H2AX MFI strongly correlated with accumulated dose ($p < 0.001$, $r = 0.71$) (Fig. 6a), while γ -H2AX foci number moderately correlated with accumulated dose ($p < 0.001$, $r = 0.55$) (Fig. 6b). Receiver operating characteristic (ROC) analysis was used to evaluate the performance (Lacombe et al. 2018) and estimate the sensitivity and specificity of γ -H2AX MFI and foci number to discriminate the “classification threshold” (e.g. 2 Gy) (PREP 2005; Sullivan et al. 2013; Williams et al. 2016). The optimal cut off value of γ -H2AX MFI and foci number were determined by Youden Index with the highest sensitivity and specificity. The sum value of MFI= 1583 for fluorescence and foci number=8.29 were used as the cut off value to determine whether the accumulated dose is higher than 2 Gy. The area under the curve (AUC) was 0.898 and 0.868 respectively, for γ -H2AX MFI (standard error [SE], 0.061; 95% confidence interval [CI], 0.776 to 1.019, $p < 0.001$) and foci number (standard error [SE], 0.102; 95% confidence interval [CI], 0.690 to 1.046, $p < 0.01$) (Fig. 6c and 6d).

Discussion

Internal radiation exposure has been considerably understudied largely due to the practicalities and expense associated with ^{137}Cs *in vivo* studies. The recent development of our ^{137}Cs VADER irradiator has allowed us to simulate protracted radionuclide exposures for measuring the DNA damage response in mouse peripheral blood leukocytes *in vivo* (Garty et al. 2017). Besides the flexibility in providing varying dose and dose rate, the advantage of the VADER lies in the availability of collecting biofluids without ^{137}Cs radioactive contamination, which allowed us to use a shared-facility imaging flow cytometry (IFC) system to rapidly measure multiple biomarker endpoints.

In the present study, leukocytes and T cell counts were significantly decreased at day 7 (total dose = 2.7 Gy), while B cells started to decrease by day 4 (dose =1.71 Gy) and remained low up to 7 days. These findings are consistent with previous work that demonstrated that B cells were more sensitive than other lymphocytes subsets in the peripheral mouse blood cell population following whole-body irradiation (Kajioka et al. 2000). The results indicated that under the protracted radionuclide exposure scenario described here, the radiation-induced decrease in leukocyte levels were apparently dependent on accumulated dose as opposed to low dose rates. Gridley et al. similarly suggested that blood leukocyte count depletion following gamma-radiation was more dependent on the accumulated dose rather than dose

rate (Gridley et al. 2001). Measurements of blood subset count *in vivo* are important physiological biomarkers for the response to ionizing radiation which could provide useful diagnostic indices to confirm individual's with severe radiation injuries and can be used in combination with high throughput blood biomarker assay systems for rapid dose determinations (Hu et al. 2015).

Previously we have shown that radiation-induced apoptosis/cell death can contribute to the depletion of the peripheral leukocytes *in vivo* (Turner et al. 2015a). The use of imaging flow technology has enabled us to acquire the percentage of the apoptotic cells according to their complexity of nucleus and contrast morphology. The results showed that the proportion of apoptotic cells was relatively low (< 3%), with no significant difference observed between the VADER irradiation group and the non-irradiated control. Activation of p53 during VADER low-dose rate irradiation exposures, showed that p53 levels in non-apoptotic leukocytes peaked at Day 2 (total dose = 0.9 Gy), and remained significantly elevated up to Day 4. As expected, p53 protein levels were consistently higher in the apoptotic cell population across the 7-day study period (data not shown). Functionally, p53 is a transcription factor with control of target genes that influence cell cycle arrest, DNA repair, apoptosis, and senescence (Eriksson and Stigbrand 2010). Depending on the extent of damaged DNA and cell type, p53 can activate elimination routes for damaged cells by apoptosis or senescence (Rodier et al. 2009; Rufini et al. 2013). Upon protracted low-dose irradiation, cells may gradually up-regulate the protective mechanisms, changes in cell turnover, apoptosis, DNA repair, intercellular communication, and/or anti-oxidation may mediate such adaptive processes (Flidner et al. 2012). We speculate that the early p53 response measured here could also lead to an increase in cell senescence, thereby preventing consequent damage from being propagated to the next cell generation, contributing to the overall leukocyte depletion by 7 days of irradiation. Similarly, Cao. et al demonstrated that the chronic *ex vivo* low-dose irradiation up to 10 days induced considerably more cellular senescence in human tumor cell lines compared with an acute dose (Cao et al. 2014).

In contrast to the p53 MFI kinetics, real-time γ -H2AX MFI and foci number showed a significant increase with accumulated dose up to day 5, which had decreased by day 7 (Fig. 5). Although both the γ -H2AX MFI and foci number increased with accumulated dose during the study period, the results showed that the goodness of fit for linear regression of γ -H2AX MFI is better than γ -H2AX foci number. This may be due to the current configuration of our ISX IFC platform which only contains a 40 \times lens for imaging acquisition. Increasing the magnification from 40 \times to 60 \times together with extended depth of field (EDF) focus stacking option could provide a more accurate assessment of foci number (Lee et al. 2019). To this end, ROC analysis showed that γ -H2AX MFI provided a better discrimination of accumulated dose < 2 Gy and \geq 2 Gy which is a "classification threshold" (PREP 2005; Sullivan et al. 2013; Williams et al. 2016) cut-off targeting those who need immediate medical intervention (Fig. 6c), suggesting that the γ -H2AX biomarker could have utility as a candidate biomarker for biological dosimetry in a protracted, environmental exposure scenario. This is consistent with recent studies suggesting that γ -H2AX MFI could be a useful biomarker for detecting low-dose radiation exposure and DNA damage repair kinetics after internal ^{131}I injection in thyroid cancer patients (Eberlein et al. 2016; Lassmann et al. 2010).

The development of radiation biodosimetry assays for rapid and accurate dose estimations are highly desired. Here, we adapted IFC technology for the γ -H2AX and p53 assay. IFC is a relatively new technology that has been developed to combine the statistical power of traditional flow cytometry with the sensitivity and specificity of microscopy acquisition speeds of 1000 cells/seconds (Wang et al. 2019). It also allows the analysis of cell morphology and quantitative multi-parametric fluorescent intensities (Vorobjev and Barteneva 2016). The application of multispectral IFC provides a novel and robust methodology for the estimation and quantitation of γ -H2AX MFI as well as foci number in cells. Recently, we have developed an IFC-based human γ -H2AX assay to measure DNA repair kinetics in human lymphocytes *ex vivo*, up to 24 h after acute exposures (Lee et al. 2019). We proposed that measurements of individual DSB repair capacity within a large population could offer valuable information to advance this high-throughput assay for translational research such as monitoring risk and response among radiotherapy patients.

In summary, we have used novel IFC technology to investigate the peripheral blood leukocyte kinetic response after exposure to external variable low-dose rate external ^{137}Cs irradiator over 7 days. The results presented here highlight the potential of γ -H2AX as a biomarker to provide a good discrimination of accumulated dose < 2 Gy and ≥ 2 Gy in a protracted, environmental exposure scenario with the long-term goal to advance the high-throughput IFC-biomarker system for large-scale biodosimetry. Follow-up studies for the development of biodosimetry biomarkers for dose and injury using our VADER irradiator for protracted exposures is needed.

Acknowledgements

We thank Bezael A. Bacon for sample measurement. We are also grateful to Matthew A. Rodrigues for valuable discussion of this work.

Funding:

This work was supported by the Center for High-Throughput Minimally-Invasive Radiation Biodosimetry, National Institute of Allergy and Infectious Diseases (grant number U19AI067773).

Reference

- Buddemeier B, Dillon M (2009) Key response planning factors for the aftermath of nuclear terrorism. Lawrence Livermore National Lab.,
- Cao L et al. (2014) A novel ATM/TP53/p21-mediated checkpoint only activated by chronic γ -irradiation. *PLoS One* 9:e104279 [PubMed: 25093836]
- Eberlein U et al. (2016) DNA damage in peripheral blood lymphocytes of thyroid cancer patients after radioiodine therapy. *J Nucl Med* 57:173–179 [PubMed: 26564321]
- Eriksson D, Stigbrand T (2010) Radiation-induced cell death mechanisms. *Tumour Biol* 31:363–372 [PubMed: 20490962]
- Fliedner TM, Graessle DH, Meineke V, Feinendegen LE (2012) Hemopoietic response to low dose-rates of ionizing radiation shows stem cell tolerance and adaptation. *Dose-Response* 10: dose-response. 12–014. Feinendegen
- Garty G, Pujol-Canadell M, Brenner DJ (2019a) An injectable dosimeter for small animal irradiations *Physics in medicine and biology* 64:18nt01 doi: 10.1088/1361-6560/ab3bb9
- Garty G, Xu Y, Elliston C, Marino SA, Randers-Pehrson G, Brenner DJ (2017) Mice and the Abomb: irradiation systems for realistic exposure scenarios. *Radiat Res* 187:475–485

- Garty G et al. (2019b) VADER: a VARIABLE Dose-rate External 137Cs irradiator for internal emitter and low dose rate studies arXiv preprint arXiv:190504169
- Goudarzi M et al. (2013) Development of urinary biomarkers for internal exposure by cesium-137 using a metabolomics approach in mice. *Radiat Res* 181:54–64 [PubMed: 24377719]
- Gridley D, Pecaut M, Miller GM, Mouers M, Nelson G (2001) Dose and Dose Rate Effects of Whole Body γ -Irradiation: II. Hematological Variables and Cytokines. *In Vivo-Attiki* 15:209–216
- Heller A (2015) Helping Cities Prepare for a Disaster. *Science and Technology Review*
- Hu S, Blakely WF, Cucinotta FA (2015) HEMODOSE: a biodosimetry tool based on multi-type blood cell counts. *Health phys* 109:54 [PubMed: 26011498]
- Kajioka EH et al. (2000) Acute effects of whole-body proton irradiation on the immune system of the mouse. *Radiat Res* 153:587–594 [PubMed: 10790280]
- Lacombe J, Sima C, Amundson SA, Zenhausern F (2018) Candidate gene biodosimetry markers of exposure to external ionizing radiation in human blood: A systematic review. *PLoS one* 13:e0198851 [PubMed: 29879226]
- Lassmann M, Hanscheid H, Gassen D, Biko J, Meineke V, Reiners C, Scherthan H (2010) In vivo formation of γ -H2AX and 53BP1 DNA repair foci in blood cells after radioiodine therapy of differentiated thyroid cancer. *J Nucl Med* 51:1318–1325 [PubMed: 20660387]
- Lee Y, Wang Q, Shuryak I, Brenner DJ, Turner HC (2019) Development of a high-throughput gamma-H2AX assay based on imaging flow cytometry. *Radiation oncology (London, England)* 14:150 doi:10.1186/s13014-019-1344-7
- López-Vicente M, Onda Y, Takahashi J, Kato H, Chayama S, Hisadome K (2018) Radiocesium concentrations in soil and leaf after decontamination practices in a forest plantation highly polluted by the Fukushima accident. *Environ Pollut* 239:448–456 [PubMed: 29679942]
- Moysich KB, Menezes RJ, Michalek AM (2002) Chernobyl-related ionising radiation exposure and cancer risk: an epidemiological review. *Lancet Oncol* 3:269–279 [PubMed: 12067803]
- Nakamura AJ et al. (2017) The causal relationship between DNA damage induction in bovine lymphocytes and the Fukushima Nuclear Power Plant Accident. *Radiat Res* 187:630–636 [PubMed: 28240558]
- Paul S, Ghandhi SA, Weber W, Doyle-Eisele M, Melo D, Guilmette R, Amundson SA (2014) Gene expression response of mice after a single dose of 137CS as an internal emitter. *Radiat Res* 182:380–389 [PubMed: 25162453]
- PREP E (2005) Generic procedures for medical response during a nuclear or radiological emergency
- Redon CE, Nakamura AJ, Gouliava K, Rahman A, Blakely WF, Bonner WM (2010) The use of gamma-H2AX as a biodosimeter for total-body radiation exposure in non-human primates. *PLoS one* 5:e15544
- Rodier F et al. (2009) Persistent DNA damage signalling triggers senescence-associated inflammatory cytokine secretion. *Nat Cell Biol* 11:973 [PubMed: 19597488]
- Rothkamm K, Horn S (2009) gamma-H2AX as protein biomarker for radiation exposure. *Ann Ist Super Sanita* 45:265–271 [PubMed: 19861731]
- Rufini A, Tucci P, Celardo I, Melino G (2013) Senescence and aging: the critical roles of p53. *Oncogene* 32:5129 [PubMed: 23416979]
- Simon SL, Bouville A, Beck HL (2004) The geographic distribution of radionuclide deposition across the continental US from atmospheric nuclear testing. *J Environ Radioact* 74:91–105 [PubMed: 15063539]
- Solier S, Pommier Y (2014) The nuclear gamma-H2AX apoptotic ring: implications for cancers and autoimmune diseases *Cellular and molecular life sciences : CMLS* 71:2289–2297 doi:10.1007/s00018-013-1555-2 [PubMed: 24448903]
- Steinhausler F (2005) Chernobyl and Goiania lessons for responding to radiological terrorism. *Health physics* 89:566–574 [PubMed: 16217200]
- Sullivan JM, Prasanna PG, Grace MB, Wathen L, Wallace RL, Koerner JF, Coleman CN (2013) Assessment of biodosimetry methods for a mass-casualty radiological incident: medical response and management considerations *Health physics* 105

- Turner H et al. (2015a) Effect of dose rate on residual γ -H2AX levels and frequency of micronuclei in X-irradiated mouse lymphocytes. *Radiat Res* 183:315–324 [PubMed: 25738897]
- Turner HC et al. (2019) Effect of dose and dose rate on temporal γ -H2AX kinetics in mouse blood and spleen mononuclear cells in vivo following Cesium-137 administration. *BMC Mol Cell Biol* 20:13 [PubMed: 31138230]
- Turner HC et al. (2014) The RABiT: high-throughput technology for assessing global DSB repair. *Radiat Environ Biophys* 53:265–272 [PubMed: 24477408]
- Turner HC et al. (2015b) gamma-H2AX Kinetic Profile in Mouse Lymphocytes Exposed to the Internal Emitters Cesium-137 and Strontium-90 *PloS one* 10:e0143815 doi:10.1371/journal.pone.0143815 [PubMed: 26618801]
- Vorobjev IA, Barteneva NS (2016) Quantitative functional morphology by imaging flow cytometry In: *Imaging Flow Cytometry*. Springer, pp 3–11
- Wang Q et al. (2019) Automated Triage Radiation Biodosimetry: Integrating Imaging Flow Cytometry with High-Throughput Robotics to Perform the Cytokinesis-Block Micronucleus Assay. *Radiat Res* 191:342–351 [PubMed: 30779694]
- Williams BB, Flood AB, Demidenko E, Swartz HM (2016) ROC analysis for evaluation of radiation biodosimetry technologies *Radiation protection dosimetry* 172:145–151 [PubMed: 27412513]
- Yasunari TJ, Stohl A, Hayano RS, Burkhart JF, Eckhardt S, Yasunari T (2011) Cesium-137 deposition and contamination of Japanese soils due to the Fukushima nuclear accident. *Proc Natl Acad Sci* 108:19530–19534 [PubMed: 22084074]

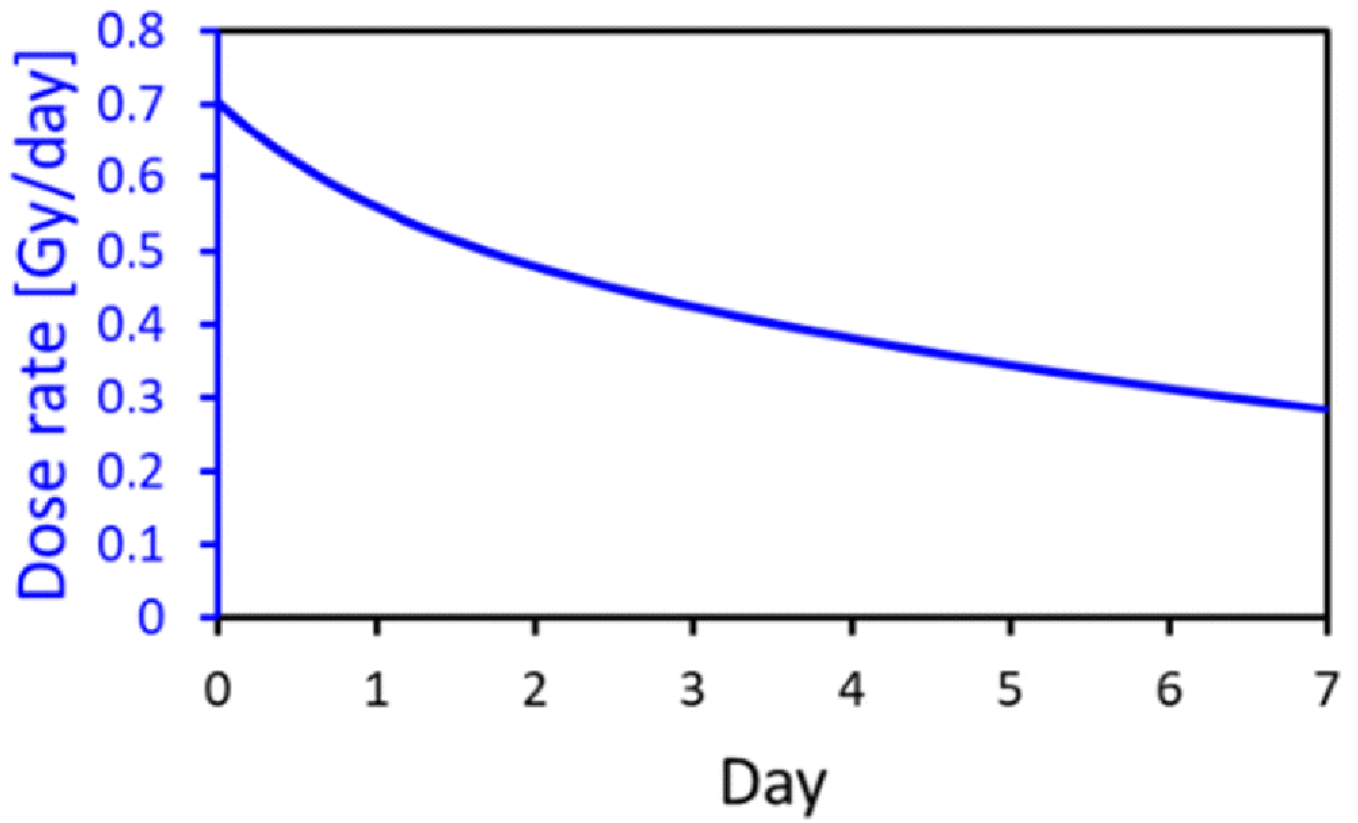


Fig. 1.
Dose rate vs time programmed into the VADER.

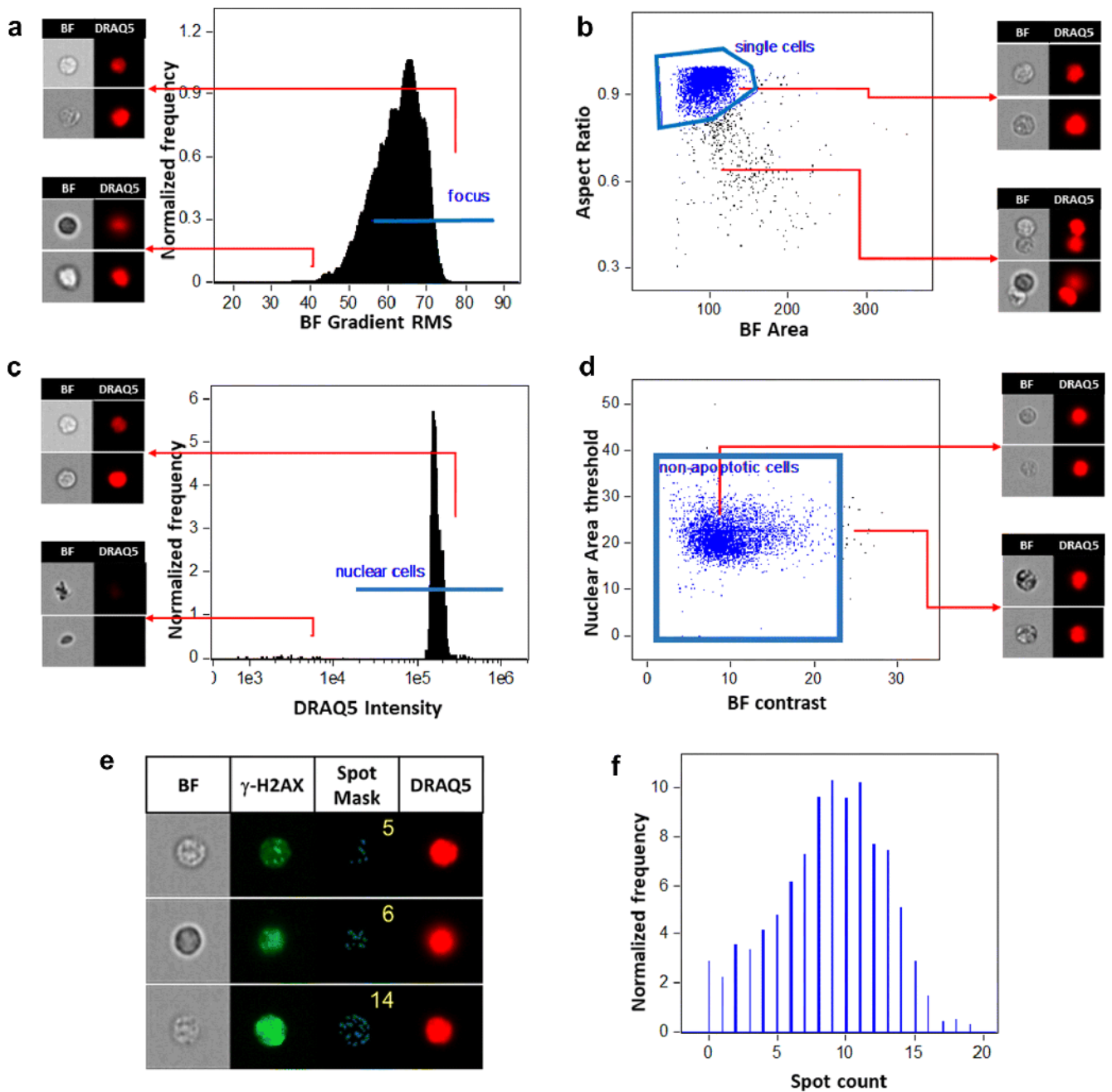


Fig. 2.

Gating strategy and the foci counting for γ -H2AX in the IDEAS® software, (a) According to the gradient similarity feature in the bright field channel, the focused cells were gated; (b) According to area and aspect ratio in the bright field channel, single cells were selected; (c) Nucleated cells are selected based on DRAQ5 positivity; (d) Non-apoptotic cells were gated according to automated image analysis based on nuclear imagery features in combination with bright field morphology, (e) Representative images of γ -H2AX foci analysis in mouse peripheral blood leukocytes. Images display cells on bright field, γ -H2AX staining, γ -H2AX foci mask, DRAQ5 nuclear staining (40x magnification). The spot counts as shown

in the spot mask column is automatically enumerated by spot counting wizard, (f) Histogram of spot count performed by wizard in the IDEAS[®] software to identify the number of γ -H2AX foci per sample. BF=Bright field.

Author Manuscript

Author Manuscript

Author Manuscript

Author Manuscript

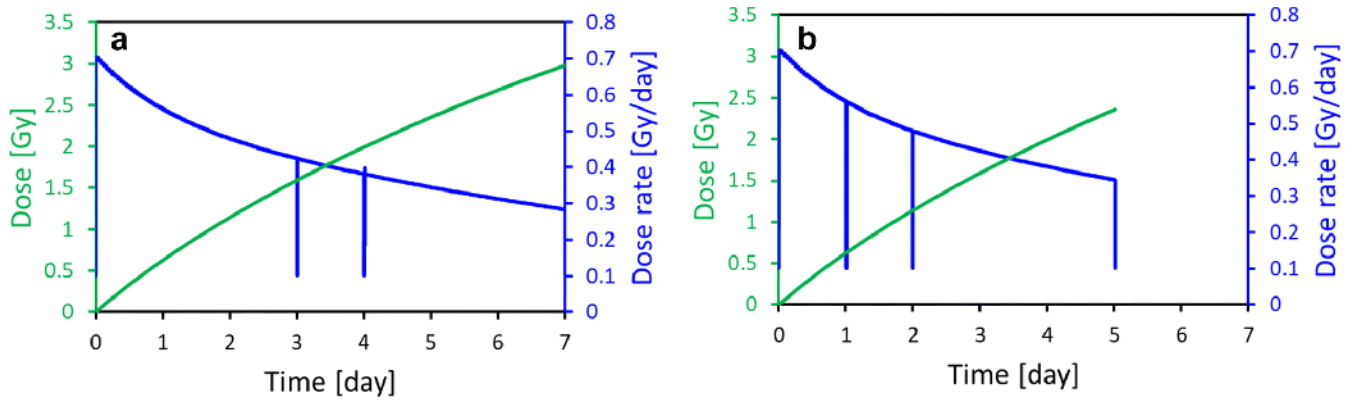


Fig. 3: Dose rate (blue), based on the measured source positions, and cumulative doses (green). The dips in the dose rate curve correspond to VADER openings, a) First batch of mice (day 3, day 4 and day 7); b) Second batch of mice (day 1, day 2 and day 5)

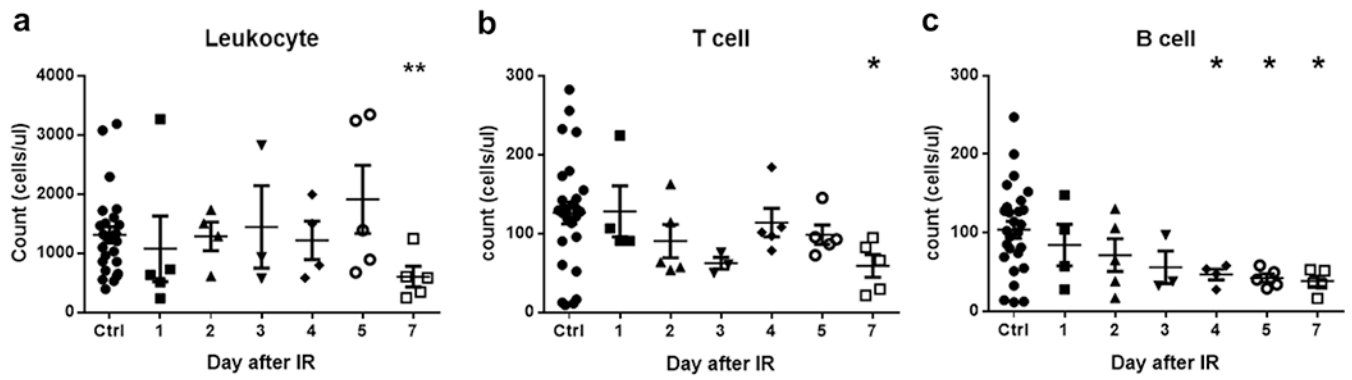
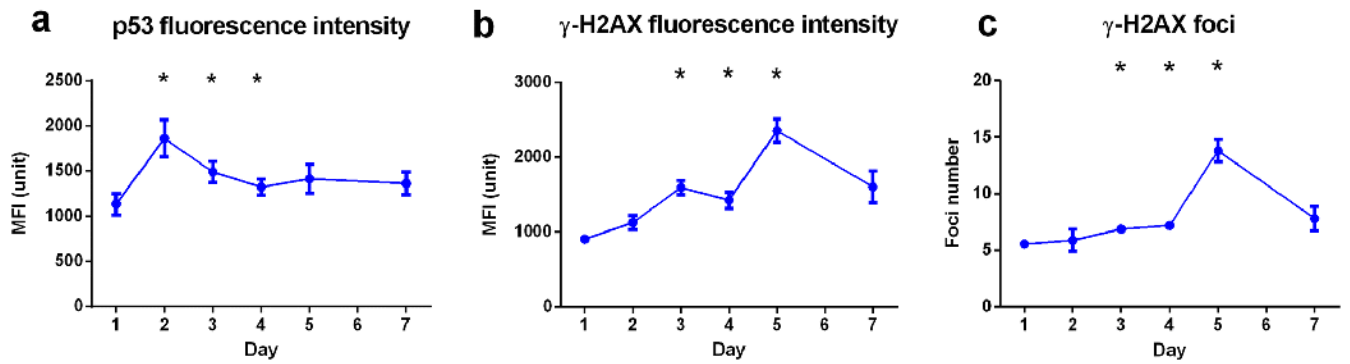


Fig. 4. Effects of VADER irradiation on peripheral blood leukocyte, T cell and B cell counts, (a) Leukocyte counts; (b) T cell counts; (c) B cells counts. Error bar is expressed in means \pm SEM. The Kruskal-Wallis test was performed to compare data among study groups. The Mann-Whitney U test was then used to compare VADER irradiated group with non-irradiated control group. *p<0.05 and **p<0.01.

**Fig. 5.**

Kinetics of p53 and γ -H2AX fluorescence and γ -H2AX foci number in peripheral blood leukocytes during VADER irradiation: a) p53 MFI, b) γ -H2AX MFI, c) γ -H2AX foci number. Error bar is expressed in means \pm SEM. The Kruskal-Wallis test was performed to compare data among study groups. The Mann-Whitney U test was used to compare VADER irradiated group with non-irradiated control group. The lines connecting the data points are shown for visualization only, to guide the eye. * $p < 0.05$.

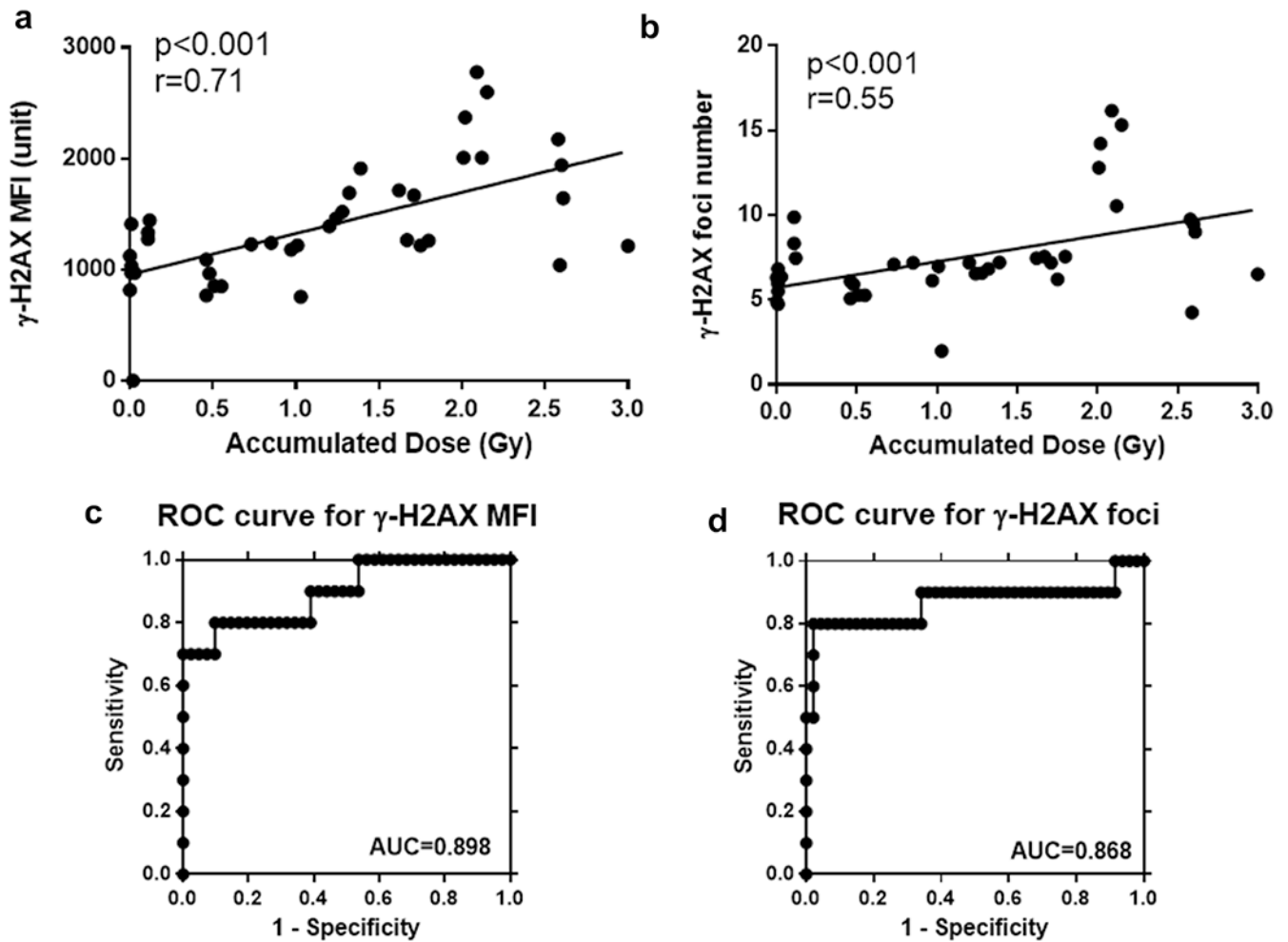


Fig. 6. Correlation of γ -H2AX mean fluorescence intensity (MFI) and foci number with accumulated dose and performance to discriminate dose, (a) Correlation of the γ -H2AX MFI with the accumulated dose ($p < 0.001$, $r = 0.71$). (b) Correlation of the γ -H2AX MFI with the accumulated dose ($p < 0.001$, $r = 0.55$). (c) Receiver operating characteristic (ROC) curve analysis to discriminate radiation dose < 2 Gy from radiation dose ≥ 2 Gy based on γ -H2AX MFI. (d) Receiver operating characteristic (ROC) curve analysis to discriminate radiation dose < 2 Gy from radiation dose ≥ 2 Gy based on γ -H2AX foci number.